Migration Letters

Volume: 21, No: S11 (2024), pp. 111-134

ISSN: 1741-8984 (Print) ISSN: 1741-8992 (Online)

www.migrationletters.com

Sediment Yield Estimation Using Gis-Based Sediment Production Rate (Spr) Approach: A Study Of Kunhar River Basin, Pakistan

Zahida Akhtar[1], Muhammad Jamal Nasir[2], Zahid Ali[3], Sardar Muzaffar Hussain Zahid[4], Shahid Iqbal[5], Zahid Khan[6]

Abstract

The Kunhar River basin (KRB) in Mansehra district, Pakistan, faces significant challenges due to soil erosion. The current study focuses on analyzing sediment production rates (SPR) in the Kunhar River basin using geographic information systems (GIS). ASTERG DEM (V3) with a spatial resolution of 30m acquired from NASA Earthdata (ASTER Global Digital Elevation Map (nasa.gov) serve as the primary source of data. The sub-basin form factor (R_f)), (Circulatory Ratio (R_c) and (Compactness Coefficient C_c) were derived using the Horton's (1945), Smith (1957), and Strahler (1964) outlined approach, in the Arc GIS 10.8 software environment. Findings reveal widespread sediment production across the basin, with certain sub-basins showing notably high rates. Th[1]e analysis reveals that the sediment production from KRB is ranging from 0.346 to 0.578 ha-m/100 km^2/year. At sub-basin level Sb-2, SB5, SB-6, SB-9, and SB-18 (24% KR sub-basins) experienced very high sediment production rate. Likewise, 11 sub-basins (52% of the KR sub-basins) i.e. SB-1, SB-4, SB-11, SB-12, SB-13, SB-14, SB-15, SB-16, SB-19, SB-20, and SB-21 have reported high levels of sediment production. The two sub-basins SB-7 and SB-8, (10% of the KR sub-basins), have a moderate sediment production rate; while; SB-3, SB-10, and SB-17, (14% of the KR sub-basins) have a low sediment production rate. These findings are crucial for policymakers and relevant organizations in making informed decisions to combat soil erosion and its adverse effects on water resources, agriculture, and infrastructure. The analysis marks a crucial step toward comprehensive watershed management strategies aimed at preserving the ecological integrity and socioeconomic resilience of the Kunhar River basin and similar hydrological systems nationwide.

Keywords: *Kunhar River Basin, Sediment Production Rate (SPR), Form Factor (F_f), Circulatory Ratio (R_c), Compactness Coefficient (C_c)*

INTRODUCTION

[1] PhD Scholar, Department of Geography, University of Peshawar, Pakistan,
[2] Assistant Professor, Department of Geography, University of Peshawar, Pakistan,
[3] Lecturer, GD College, Akbarpura, Nowshera, Pakistan. Corresponding Author,
[4] PhD Scholar, Center for Disaster Preparedness and Management, University of Peshawar.
[5] Center for Disaster Preparedness and Management, University of Peshawar.
[6] Lecturer, Department of Geography, University of Peshawar, Pakistan.
Corresponding author drjamal@uop.edu.pk

Being a major issue pertaining to agriculture sustainability, soil quality, and health have attracted significant national and worldwide interest (Panagos et al., 2018). Soil and land degradation is a common problem that harms the well-being of the environment and leads to the depletion of natural resources (Arabameri et al., 2018: Wang et al., 2020; Li et al., 2021). Soil erosion is one of the most serious issues, which reduces soil productivity by removing the topmost layer of soil. It not only influences agricultural production but also alters the area's land use land cover (LULC) (Pham et al., 2018; Tsegaye, 2019). Fluvial erosion comprises the removal, trapping, transit, and deposition of soil particles as the outermost earth's layer is eroded away by the combined power of gravity and water (Saha et al., 2018). This series of events takes place at numerous spatial and temporal scales. An estimated 15.5 billion metric tons of terrigenous sediment are annually transported to the oceans by the rivers. According to Ghabbour et al., (2017) agricultural soil erosion in the United States leads to a loss of an average of 30 tons/ha of soil each year, which is nearly eight times faster than the rate of soil formation. According to Singh and Singh (2018), average soil loss in the majority of agricultural soil has already been determined to be higher than the acceptable rate of 1 ton/ ha/year-1. According to Panagos et al., (2018) approximately 12.7% of Europe's entire land mass is at risk of moderate to severe soil erosion. The European Union's average yearly soil loss is estimated to be 970 Mt/year. Around 30% of the global agricultural land has already been lost to excessive soil erosion and transformed into unproductive land (Jahun et al., 2015). Soil loss is anticipated to get worse under the influence of climate change in areas where it currently occurring (Li and Fang, 2016; Rumpel, 2022).

Several techniques are currently established for evaluating and analyzing the rate of soil erosion on a national and international scale. Several soil erosion equations have been successfully integrated with Geographic Information System, including different variant of the Universal Soil Loss Equation (USLE), established by Wischmeier and Smith (1978). Various variants of the USLE are available i.e. Revised Universal Soil Loss Equation (RUSLE) (Das et al., 2020), RUSLE with the Sediment Delivery Ratio (RUSLESDR), Sediment Delivery Distribution Model (SEDD) (Achu & Thomas, 2023), Besides some other important field scale soil erosion models are Erosion-Productivity Impact Calculator (EPIC) (Williams, 1985), European soil Erosion Model (EUROSEM) (Morgan et a., 1998) and Water Erosion Prediction Project (WEPP) (Flanagan & Nearing, 1995).

The USLE and the RUSLE are among the most popular and widely used empirical equations for calculating yearly soil loss. Since the USLE was initially established for cropland erosion assessment, it is usually inadequate for regional-level erosion modeling (Foster and Wischmeier 1974; Moore and Wilson 1992). A large number of these quantitative models are lumped models created with statistical regression formulas (Merritt et al., 2003; Haregeweyn, 2006). However, due to the lumped model's embedded constraints, the geographical makeup of land use land cover and topography within the basin cannot be considered. Current soil loss estimation approaches rely upon the single stream power idea, which takes into account the influence of terrain shape which renders them easier to use at the sub-watershed level (Moore and Burch 1986; Mitasova and Iverson 1992).

The watershed morphometry and drainage network assessment provide a complete comprehension of the geo-hydrological behavior of the watershed and express the prevalent climatic, geological, geomorphic, and morphological characteristics of the watershed, which is particularly crucial for determining watersheds susceptible to soil erosion (Pande et al., 2021; Bharath et al., 2021; Mishra et al., 2023). Watershed morphometry is one of the most widely used Multi Criteria Decision Making (MCDM) approach, and it provides a comparable estimate based on scientific knowledge and comprehension of a qualitative phenomenon

(Todorovski & Deroski, 2006). Sustainable use of water and soil seeks to prevent soil loss and subsequent sedimentation in dams by managing the source and rate of deposition (Misra et al., 1984). The Sediment Production Rate (SPR) can be correctly predicted utilizing a multi-influencing factor (MRA) approach that incorporates various basic, relief and morphological parameters. Some geo-morphometric characteristics, including the form factor, circularity ratio and compactness coefficient, control the pace and extent of sediment generation (Fenta et al., 2017).

Multiple studies in Pakistan have been undertaken to predict the yearly rate of soil erosion employing the Revised Universal Soil Loss Equation and its various variants in the geospatial environment. Ullah et al., (2018) projected a yearly soil loss of 97.81 million tons/hectare/year in the Chakwal district of Punjab province. Maqsoom et al., (2020) estimated an annual soil loss of 58 tons/ha/year in the Chitral River basin. Soil loss in the Potohar region is expected to be 148 tons/ha/year (Batool et al., 2021).

Due to the area's steep topography and heavy precipitation, soil erosion is a serious problem in the Kunhar River basin. Erosion is a major concern due to the unstable soils and steep slopes, which can have detrimental effects on the environment and the economy. As erosion reduces soil fertility and nutrient availability, the loss of topsoil can have a substantial effect on agricultural production. Furthermore, sediment deposition in the water bodies brought on by soil erosion can harm aquatic ecosystems and the quality and quantity of water. The river Kunhar is a significant tributary of the Jhelum River system, which delivers over 11% of the total inflow in the Mangla reservoir, built on the river Jhelum (Mahmood et al., 2016). The Kunhar river alone deposits more than 0.1 million tons of sediment annually in the Mangla Reservoir. The river has the highest suspended sediment concentration compared to any river in Khyber Pakhtunkhwa, measuring 5.21gm/L, 2.75 gm/L, and 1.92 gm/L in spring, summer, and winter respectively (Sabir et al., 2012). The reservoir's water holding capacity is drastically reduced due to heavy sedimentation. Therefore, the present study is devised to estimate the sediment production at sub-watershed level using a morphometric-based Sediment Production Rate (SPR) approach in a geospatial environment.

Study Area

The Kunhar River basin (KRB) encompasses an area of around 2,600 $Km^{2,}$ is located in the Mansehra District, Khyber Pakhtunkhwa province, Pakistan. Geographically the Kunhar river watershed lies between 34°02′15″ to 35°06′ 30″ North latitude and 73°16′ 32″ to 74° 02′ 43″ East longitude (Mahmood et al., 2016). The Basin height varies from 672-meter to 5192 meters above sea level (Akbar et al., 2020). The watershed has 53% average slope. The Kunhar River is a significant river flowing from north to south for a distance of 171 km. The Kunhar Headwaters in the Himalayan peaks of the Kaghan Valley and empties into the Siran, the Lora, and other rivers as it passes through the Mansehra District. The river then continues through the Hazara region before eventually joining the Jhelum River close to Mangla (Mahmood et al., 2016). The KRB experiences a humid, subtropical climate. The mean annual temperature of the Kunhar basin is 13°C. The average annual precipitation received by KRB is 1500 mm, having two peaks. The upper part of the basin experience its first peak in March due to western disturbances. The second peak mostly occur in the lower part of the basin brought on by summer monsoon in July. The upper part of the basin however is rain shadow during summer (Mehmood et al., 2015).

Agriculture is an important economic activity. The region is peFfect for agriculture due to its rich soils and ample supply of water from the Kunhar river and its tributaries. A considerable part of the local population receives employment and earnings from farming, which is a vital

component of the watershed. Unfortunately, the region is also susceptible to severe soil erosion and a variety of natural hazards including landslides and flash floods, which can have a serious influence on agricultural output.

Material and Methods

Data Collection

The terrain of an area is precisely represented by the Digital Elevation Model (DEM). Quick morphometry is enabled by DEM-based geospatial drainage network extraction and watershed delineation (Kacem et al., 2014). DEM could be effectively used to determine many fundamental and secondary morphometric characteristics of the watershed (Buccolini et al., 2012; Nasir et al., 2023). ASTERG DEM (V3) with a spatial resolution of 30m acquired from NASA Earthdata (ASTER Global Digital Elevation Map (nasa.gov) will serve as the primary source of data.

Data Analysis

Sediment Production Rate (SPR)

Using Horton's (1945), Smith (1957), and Strahler (1964) outlined approach, the fundamental and secondary morphometric parameters were derived in the Arc GIS 10.8 software environment. The sub-basin (form factor (R_f)), (Circulatory Ratio (R_c) and (Compactness Coefficient C_c) were derived using the formulas shown in Table 1 and methodology expressed in Figure 2.

Table 1 Morphometric Parameters, definition and there empirical formulas

S.No	Parameter	Definition	Formula
Form Factor (F_f)	The ratio of the basin area to the square of the Watershed length	$F_f = (A/L_b^2)$	Horton (1945)
Circulatory Ratio (R_c)	the ratio of basin area (Au) to the area of a circle (Ac) whose perimeter is the same as the perimeter of the Watershed	$R_c = 4\pi A/P^2$ where $\pi = 3.14$	Miller (1953)
Compactness Coefficient (Cc)	The ratio of the watershed perimeter to the circumference of a comparable Circular are	$C_c = (P/2(\pi A)^{0.5})$	Horton (1945)

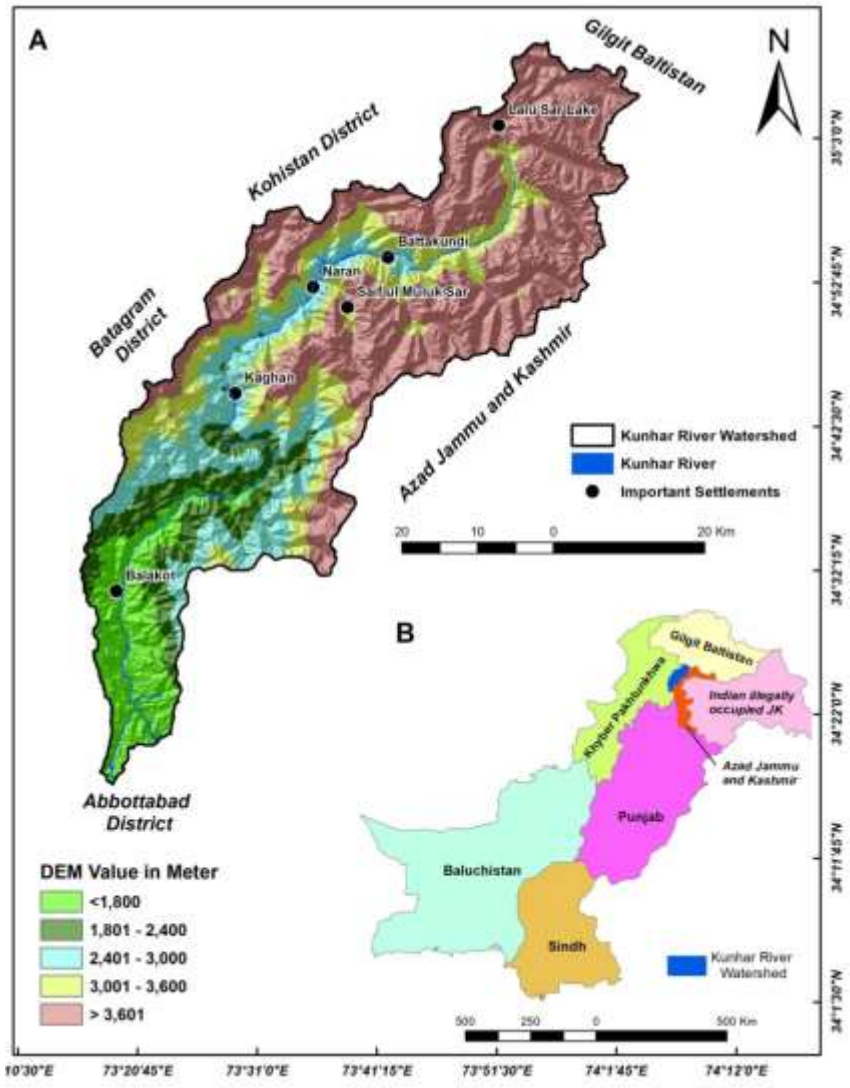

Figure 1. A. Location map of the study area Kunhar River Basin B. Pakistan Administrative Units showing location of Study area.

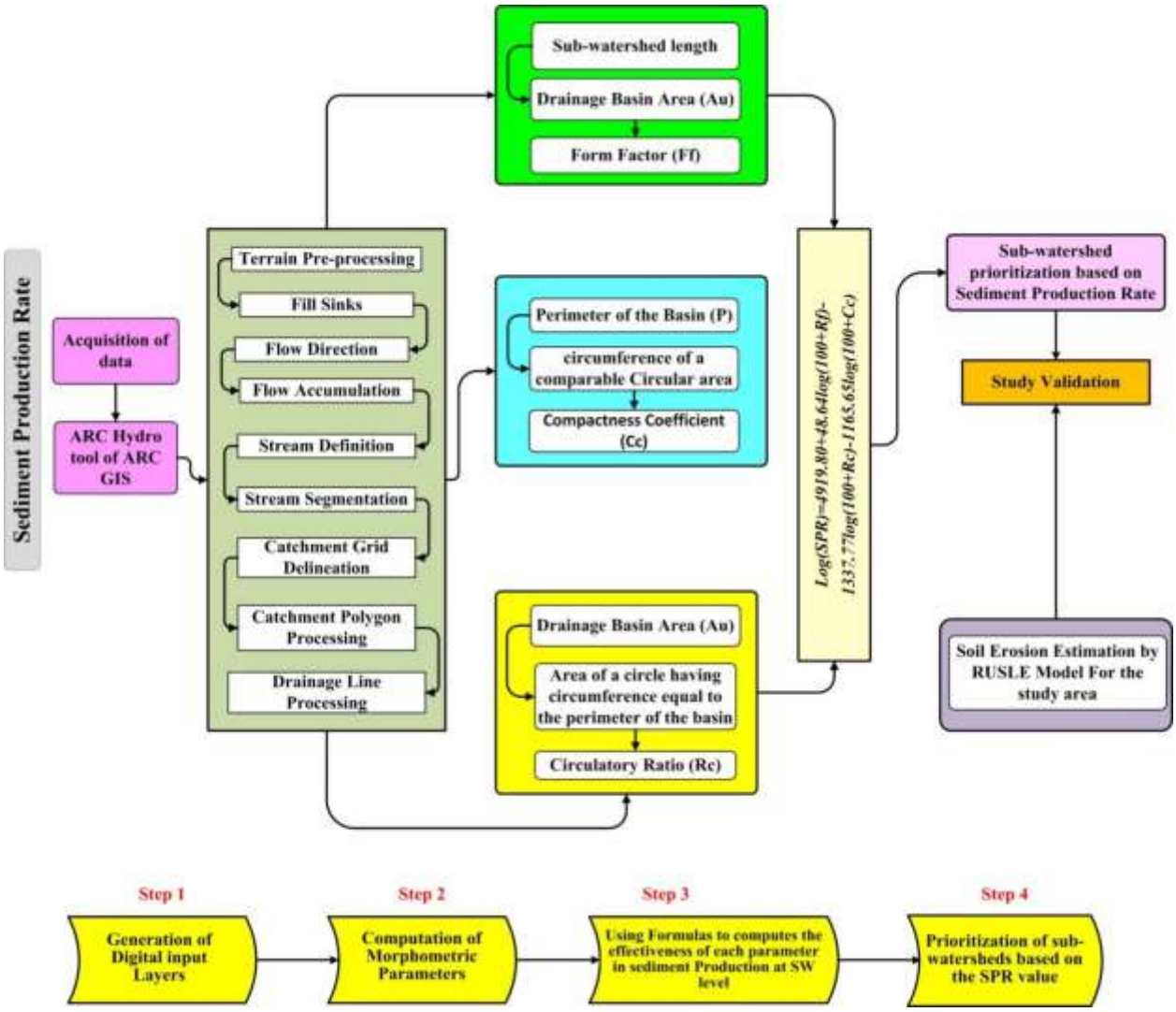

Figure 2. Research Methodology Flow Chart

Results and Discussions

Table 2 depicts the sub-basin form factor, circulatory ratio, and compactness coefficient of the Kunhar River basin. Figure 3 depicts the sub-basin form factor, circulatory ratio, and compactness coefficient graphically. Figures 4A, 4B, and 4C illustrate the spatial distribution of sub-basins form factor, circulatory ratio, and compactness coefficient of the Kunhar river basin.

Form Factor (F_f)

The "form factor" is a geometric parameter in morphometric analysis that is used to describe the geometry of a drainage basin. It is a dimensionless ratio that is computed by dividing the basin's area (A) by the square of the basin length (L_b^2). Equation 3 is a mathematical expression for the form factor (F_f):

$$Form\ Factor = \frac{A}{Lb^2} \ldots\ldots\ldots\ldots\ldots Eq.1$$

$$Where\ A\ is\ the\ basin\ area\ and\ Lb2\ is\ the\ square\ of\ the\ basin\ length$$

The form factor provides valuable information about the compactness or elongation of the basin shape. It is particularly useful in hydrological and geomorphological studies for understanding basin morphology, streamflow characteristics, sediment transport, and erosion processes (Meshram et al., 2020).

The form factor has several distinct value ranges. The form factor varies from 0 to 1 where a lower value is indicative of elongated basins and higher values suggest circular basins (Abboud and Nofal 2017; Sukristiyanti et al., 2018). The form factor ranges from <0.78 (elongated) to >0.78 (circular) (Vinutha and Janardana 2014; Rai et al., 2017). A watershed that is circular has high peak flows for a shorter period, whereas an extended watershed has low peak flows for a longer period. Generally speaking, circular basins feature consistent flow patterns and effective drainage characteristics. In circular basins, topographic features like ridges, valleys, and hills lopes can affect complex drainage patterns and stream flow paths.

Form factor is used in hydrological modeling to estimate various basin characteristics such as mean annual runoff, flood potential, and response to rainfall events (Kulimushi et al., 2021). It helps in understanding the relationship between basin shape and hydrological processes. Form factor influences the distribution of flow and sediment within a basin, affecting erosion and sediment transport patterns. Basins with higher form factors (more elongated shapes) may experience different erosion and sedimentation dynamics compared to circular basins.

Table 2 depicts the form factor (F_f) of 21 sub-basin of Kunhar River Basin. Figure 3 represents the sub-basins form factor value graphically. Figure 4A shows the spatial distribution of the form factor of various sub-basins in the Kunhar River basin. The analysis reveals that the sub-basin form factor varies from 0.0838 to 0.9801. According to the analysis of the form factor values the SB-14 is a more circular basin, with a farm factor value of 0.9801 and SB-15 is the more elongated basin with a farm factor value of 0.0838. The average form factor value of the Kunhar River sub-basins is 0.43.

Circulatory Ratio (R_c)

The circulatory ratio is a geo-morphometric parameter used to define a basin's or watershed's morphology. It is defined as the ratio of the circumference of a circle with the same area as the watershed to the actual perimeter of the watershed (Miller, 1953). The circulatory ratio is a dimensionless morphometric parameter that is used to measure the period of concentration. It is also referred to as the Horton number or Horton index. Mathematically, it can be expressed as equation 4.4:

$$Circulatory\ Ratio(R_c) = \frac{4\pi A}{P^2} \ldots\ldots\ldots\ldots\ldots Eq.2$$

$$Where\ \boldsymbol{A}\ is\ the\ area\ of\ the\ sub-basin$$

$$\boldsymbol{P}\ is\ the\ perimeter\ of\ the\ sub-basin\ and$$

$$\boldsymbol{\pi}\ is\ the\ mathamatical\ constant\ (approximatly\ 3.14159)$$

The circulatory ratio sheds light on the watershed's elongation or compactness. Greater circularity is indicated by a number nearer 1, whereas greater elongation or irregularity is indicated by a value farther from 1 (Hembran and Saha 2020). The ability to characterize the geometry of a watershed is particularly helpful in hydrological and geomorphological investigations since it affects several elements such as runoff generation, soil erosion, sediment

transport, and drainage patterns (Haokip et al., 2022). A watershed's time of concentration, the amount of time it takes for water to move from a remote location to the outlet—is influenced by the circulatory ratio. It essentially represents the ratio of the maximum to the minimum travel times of water within the watershed.

The circulatory ratio typically ranges between 0 to 1. Generally speaking, the low, moderate, and high R_c values suggest the young, mature, and old state of the development of the respective watershed (Wilson et al., 2012). According to Parkash et al., (2019), the basins/watersheds with the circulatory ratio of 0.4 to 0.7 are indicative of a more elongated basin having a homogenous lithology. The late maturity stage of the basin's topography is indicated by the high circularity ratio value.

The circulatory ratio computed for 21 sub-basins of the Kunhar River basin is shown in Table 2 and represented graphically in Figure 3. Figure 4B illustrates the spatial distribution of the sub-basin circulatory ratio of the Kunhar River basin. The analysis suggests that the R_c value of the Kunhar River sub-basins varies between 0.3377 and 0.7209. The highest R_c value is computed for SB-11 (0.7209), and the lowest for SB-1 (0.3377). The average R_c value of the Kunhar River sub-basins is 0.52.

Compactness coefficient (C_c)

The compactness coefficient in morphometric analysis is employed to quantify a basin's extent of compactness or circularity. It is computed by dividing the basin's area by its circumference or perimeter. It is the ratio of the watershed perimeter to the circumference of a comparable Circular area. The compactness coefficient can be stated quantitatively as follows in equation 3 (Horton, 1945):

$$Cpompactness\ Coefficient\ (C_c) = ({}^{P}/_{2(\pi A)^{0.5}}) \dots\dots\dots\dots\dots\dots Eq.3$$

$$Where\ P\ is\ the\ sub-basin\ perimeter\ and\ \boldsymbol{A}\ is\ the\ area\ of\ the\ watershed$$

Compactness coefficient values normally lie in the range of 0 to 1. A value nearer 1 denotes a more condensed or round basin, whereas a value nearer 0 denotes a more extended or uneven shape of basin. This metric is frequently used in morphometric analysis to measure the basin/watershed's shape attributes. The compactness coefficient has the potential to affect soil erosion processes by influencing the structure and hydraulic characteristics of the soil (Ganie et al., 2023). The compactness coefficient of a basin determines the soil permeability, and this can ultimately determine how vulnerable the soil is to erosion. Higher compaction coefficient soils typically have more compact structures with smaller pore gaps. Higher erosion rates may result from this denser structure's ability to obstruct water infiltration and enhance surface runoff, particularly during periods of intense rainfall.

The ability of soil to carry water is known as hydraulic conductivity, and it can be influenced by the compactness coefficient. The compact and hard soils usually have poor hydraulic conductivity due to the smaller pore spaces and higher soil density. Because of its lower permeability, erosion may be accelerated by surface runoff as compared to the soil with higher penetration potential (Benzougagh et al., 2022). Although soil erosion rates may not be directly determined by the compactness coefficient, it does have an impact on surface roughness, soil structure, and hydraulic properties—all of which are critical elements that increase the susceptibility of soil erosion. In practice, the basin's compactness coefficients can help in understanding the rate and intensity of soil erosion processes operation in a

basin/watershed and turn can be useful in erosion control techniques and soil management practices that aim to reduce erosion risk.

Table 2 depicts the Sub-basins Compactness Coefficient (C_c) of the Kunhar River Basin. Figure 3 is the graphical representation of the sub-basins compactness coefficient of the Kunhar River basin and Figure 4C illustrates the compactness coefficient of 21 sub-basins of Kunhar River basins. The analysis reveals that the average C_c value for the Kunhar River basin is moderate to high i.e. 0.6439. The majority of the lower basins have higher C_c values compared to the upper basins. The highest Cc value is computed for SB-18 (0.9429) and the lowest for SB-1 (0.3446). The higher C_c value suggests a higher runoff and less infiltration capacity of the basin thus having a high susceptibility to soil erosion. Keeping in view the higher C_c values of SB-11, SB-18, SB-19, and SB-20 suggest a higher risk of soil erosion.

Table 2 The sub-basins form factor, circulatory ratio, and compactness coefficient of the Kunhar river basin.

Sub-basins	**Form Factor**	**Circulatory Ratio**	**Compactness Coefficient**
	$\mathbf{F_f = A/Lb^2}$	$\mathbf{R_c = 4\pi A/P^2}$	$\mathbf{(C_c) = (P/2(\pi A)^{0.5})}$
SB-1	0.4322	0.3377	0.3446
SB-2	0.7393	0.4980	0.5192
SB-3	0.2812	0.4781	0.5500
SB-4	0.4357	0.5337	0.6058
SB-5	0.3604	0.5276	0.5757
SB-6	0.4589	0.4750	0.5100
SB-7	0.3916	0.4659	0.5014
SB-8	0.2874	0.4697	0.6122
SB-9	0.3330	0.4202	0.4663
SB-10	0.3286	0.4974	0.6617
SB-11	0.5409	0.7209	0.9021
SB-12	0.3179	0.4896	0.6400
SB-13	0.3688	0.5494	0.6182
SB-14	1.3047	0.5038	0.6469
SB-15	0.0838	0.5745	0.7735
SB-16	0.4059	0.4990	0.6941
SB-17	0.2841	0.5507	0.7684
SB-18	0.4493	0.6230	0.9429
SB-19	0.3606	0.5879	0.7410
SB-20	0.5610	0.6590	0.8180
SB-21	0.2764	0.4095	0.5407
Average	0.4387	0.5176	0.6396

Source: Analysis in ArcMap 10.8

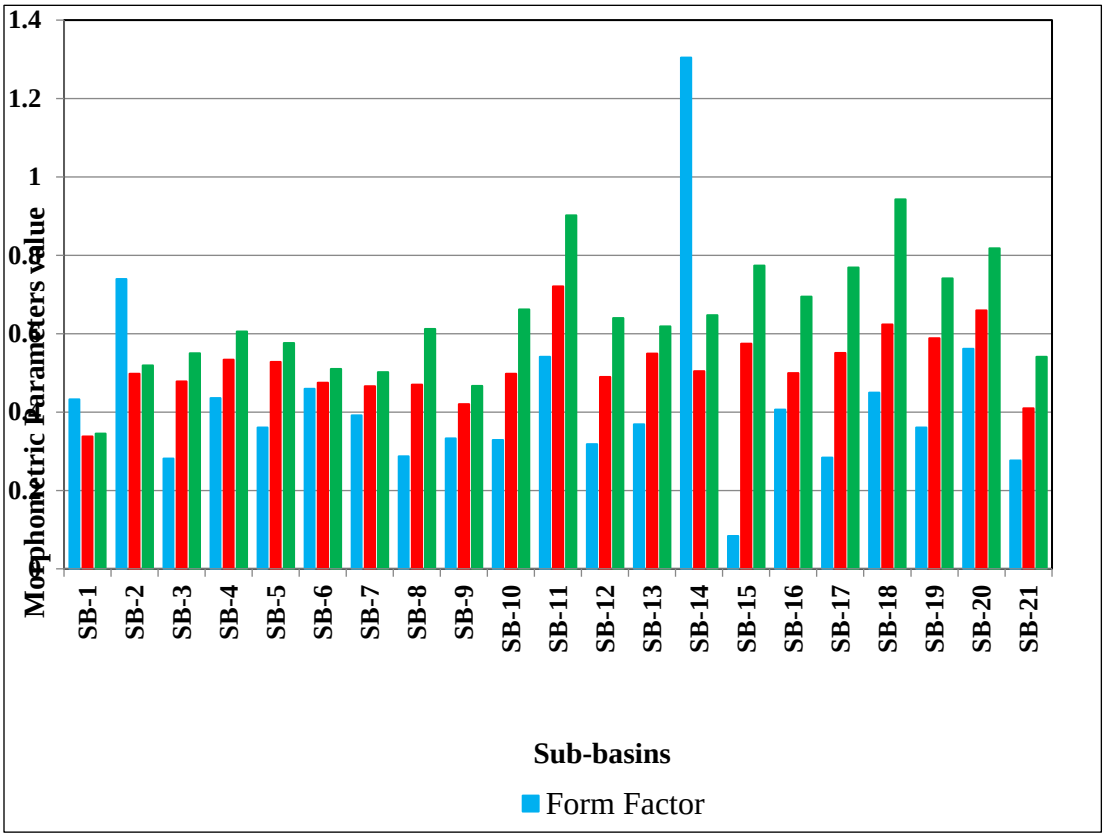

Figure 5.1 Showing sub-basins form factor, circulatory ratio and compactness

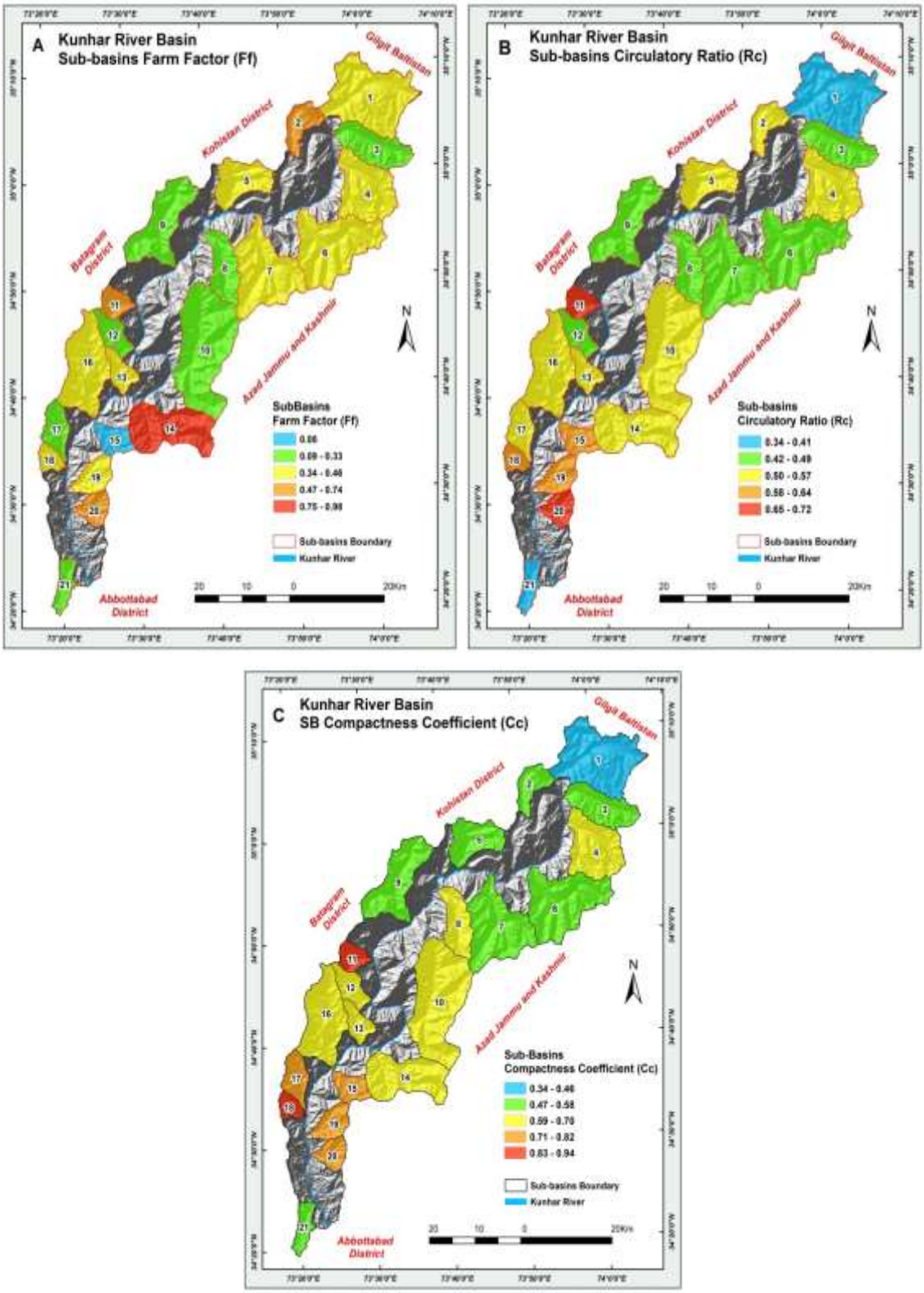

Figure 4 illustrating the sub-basins ***(A)*** form factor (F_f) of Kunhar river basin, ***(B)*** the sub-basins Circulatory Ratio (R_c) and ***(C)*** the sub-basins Compactness Coefficient (C_c)

Sediment Production Rate

Sediment production rate refers to the rate at which sediment, such as sand, silt, and clay particles, are eroded and transported by natural processes like wind, water, and ice. This rate can vary significantly depending on factors such as the type of terrain, climate, vegetation cover, and human activities in the basin/watershed.

By controlling the origin and rate of sediment generation, soil and water conservation seeks to reduce soil loss and the resulting sedimentation (Misra et al., 1984). The (form factor (F_f)), Circulatory Ratio (R_c) and Compactness Coefficient (C_c)˙ among other geo-morphometric variables, control the rate and intensity of sediment generation (Fenta et al., 2017). Kulimushi et al., (2021) expressed the sediment Production Rate (SPR) empirically as follows in equation 4:

$$\text{Log(SPR)} = 4919.80 + 48.64\log(100 + \text{Ff}) - 1337.77\log(100 + \text{Rc}) - 1165.65\log(100 + \text{Cc}) \ldots\ldots\ldots\ldots\ldots\ldots \text{Eq. 4}$$

$$\text{Where log SPR is the Sediment Production Rate, (ha} - \text{m}/100\text{km}^2/\text{year}, \text{F}_\text{f} = \dot{\text{F}}\text{orm Factor}, \text{R}_\text{c} = \text{Circulatory ratio and C}_\text{c} = \text{Compactness Coeffiecient}$$

Utilizing equation 4 the sediment production rate for sub-basins of the Kunhar river basin is computed. The computed results are summarized in Table 3A (Form Factor), 3B (Circulatory Ratio), 3C (Compactness Coefficient), and Table 3D (Sub-basin Sediment Production rate). Figure 5 depicts the sub-basins-wise sediment production rate and their relative percentage. Figure 6 illustrates the spatial distribution of the sub-basin sediment production rate of the Kunhar River basin. The analysis suggests that there is a very high sediment production rate in five sub-basins i.e. Sb-2, SB5, SB-6, SB-9, and SB-18; these five sub-basins make up 24 percent of the total Kunhar River sub-basins. Likewise, 11 sub-basins (representing 52% of the Kunhar river sub-basins) namely SB-1, SB-4, SB-11, SB-12, SB-13, SB-14, SB-15, SB-16, SB-19, SB-20, and SB-21 have reported high levels of sediment production. Of the entire Kunhar River sub-basins, two sub-basins SB-7 and SB-8, have a moderate sediment production rate (10% of the sub-basins); the other three, SB-3, SB-10, and SB-17, account for 14% of the sub-basins and have a low sediment production rate.

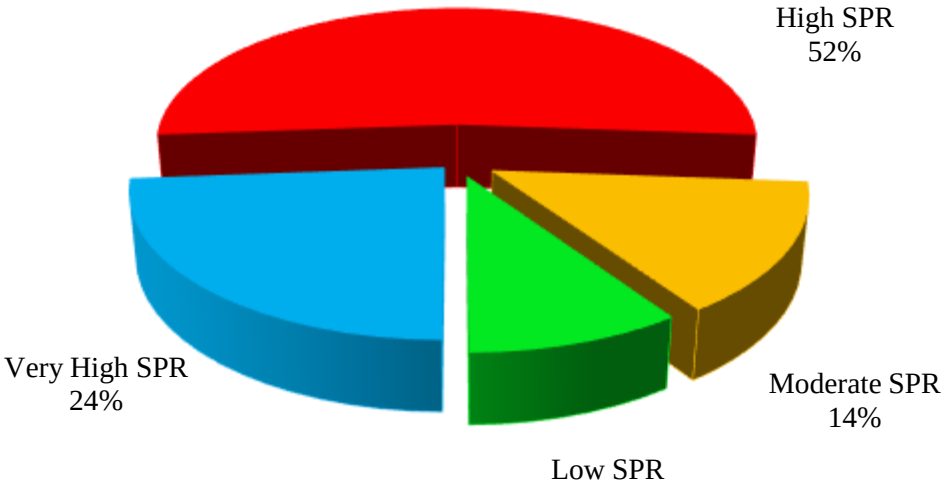

Figure 5 Percentage wise SPR of Kunhar river sub-basins

$$4919.80 + 48.64 \log(100 + Ff)$$

SB	Constant (A)	SB Farm Factor (B)	100+F_f (C)	Log of 100+F_f (D)	Constant (E)	48.64×D (Log of 100+F_f) (F)	A(4919.8)+F (G)
SB-1	4919.8	0.43221	100.43	2.0019	48.64	97.3711	5017.1711
SB-2	4919.8	0.83928	100.84	2.0036	48.64	97.45655	5017.2566
SB-3	4919.8	0.48125	100.48	2.0021	48.64	97.38141	5017.1814
SB-4	4919.8	0.49967	100.50	2.0022	48.64	97.38529	5017.1853
SB-5	4919.8	0.22491	100.22	2.0010	48.64	97.32746	5017.1275
SB-6	4919.8	0.45887	100.46	2.0020	48.64	97.37671	5017.1767
SB-7	4919.8	0.39163	100.39	2.0017	48.64	97.36257	5017.1626
SB-8	4919.8	0.28740	100.29	2.0012	48.64	97.34062	5017.1406
SB-9	4919.8	0.33303	100.33	2.0014	48.64	97.35023	5017.1502
SB-10	4919.8	0.32862	100.33	2.0014	48.64	97.3493	5017.1493
SB-11	4919.8	0.44092	100.44	2.0019	48.64	97.37294	5017.1729
SB-12	4919.8	0.31787	100.32	2.0014	48.64	97.34704	5017.1470
SB-13	4919.8	0.34000	100.34	2.0015	48.64	97.3517	5017.1517
SB-14	4919.8	0.30467	100.30	2.0013	48.64	97.34426	5017.1443
SB-15	4919.8	0.08381	100.08	2.0004	48.64	97.2977	5017.0977
SB-16	4919.8	0.40590	100.41	2.0018	48.64	97.36557	5017.1656
SB-17	4919.8	0.36000	100.36	2.0016	48.64	97.35591	5017.1559
SB-18	4919.8	0.44927	100.45	2.0019	48.64	97.37469	5017.1747
SB-19	4919.8	0.36060	100.36	2.0016	48.64	97.35604	5017.1560
SB-20	4919.8	0.56102	100.56	2.0024	48.64	97.39818	5017.1982
SB-21	4919.8	0.24639	100.25	2.0011	48.64	97.33198	5017.1320

Source: ArcMap and MS Excel analysis

Table 3B Sub-basin Circulatory Ratio values and Sediment Production Rate (SPR)
$1337.77 \log(100 + Rc)$

SB	SB Circulatory Ratio (A)	100+A (R_c) (B)	Log of B (100+R_c) (C)	Constant (D)	C×D (1337.77)
SB-1	0.513099	100.51	2.0022	1337.77	2678.5134
SB-2	0.446819	100.45	2.0019	1337.77	2678.1302
SB-3	0.354388	100.35	2.0015	1337.77	2677.5953
SB-4	0.527045	100.53	2.0023	1337.77	2678.5940
SB-5	0.560297	100.56	2.0024	1337.77	2678.7862
SB-6	0.36038	100.36	2.0016	1337.77	2677.6300
SB-7	0.504623	100.50	2.0022	1337.77	2678.4644
SB-8	0.352132	100.35	2.0015	1337.77	2677.5822
SB-9	0.606452	100.61	2.0026	1337.77	2679.0528
SB-10	0.464002	100.46	2.0020	1337.77	2678.2296
SB-11	0.39287	100.39	2.0017	1337.77	2677.8180
SB-12	0.401067	100.40	2.0017	1337.77	2677.8655
SB-13	0.49997	100.50	2.0022	1337.77	2678.4375
SB-14	0.410147	100.41	2.0018	1337.77	2677.9180
SB-15	0.46	100.46	2.0020	1337.77	2678.2064
SB-16	0.360445	100.36	2.0016	1337.77	2677.6304
SB-17	0.458829	100.46	2.0020	1337.77	2678.1996
SB-18	0.492442	100.49	2.0021	1337.77	2678.3940
SB-19	0.424516	100.42	2.0018	1337.77	2678.0012
SB-20	0.550106	100.55	2.0024	1337.77	2678.7273
SB-21	0.304838	100.30	2.0013	1337.77	2677.3084

Source: ArcMap and MS Excel analysis

Table 3C Sub-basin Compactness Coefficient values and Sediment Production Rate (SPR) 1165.65 log (100 + Cc)

SB	Compactness coefficient (C_c) (A)	$100+C_c$ (B)	log of B ($100+C_c$) (C)	Constant (D)	C× D (1165.65) (E)
SB-1	0.86	100.86	2.0037	1165.65	2335.6439
SB-2	0.80	100.80	2.0035	1165.65	2335.3385
SB-3	1.10	101.10	2.0048	1165.65	2336.8381
SB-4	0.80	100.80	2.0035	1165.65	2335.3527
SB-5	0.70	100.70	2.0030	1165.65	2334.8256
SB-6	0.90	100.90	2.0039	1165.65	2335.8357
SB-7	0.97	100.97	2.0042	1165.65	2336.1868
SB-8	1.20	101.20	2.0052	1165.65	2337.3387
SB-9	0.66	100.66	2.0029	1165.65	2334.6335
SB-10	0.99	100.99	2.0043	1165.65	2336.3062
SB-11	0.99	100.99	2.0043	1165.65	2336.2926
SB-12	0.99	100.99	2.0043	1165.65	2336.3084
SB-13	0.85	100.85	2.0037	1165.65	2335.5913
SB-14	1.00	101.00	2.0043	1165.65	2336.3184
SB-15	0.91	100.91	2.0039	1165.65	2335.8669
SB-16	1.05	101.05	2.0045	1165.65	2336.5878
SB-17	1.00	101.00	2.0043	1165.65	2336.3372
SB-18	0.82	100.82	2.0035	1165.65	2335.4342
SB-19	0.97	100.97	2.0042	1165.65	2336.1868
SB-20	0.80	100.80	2.0035	1165.65	2335.3363
SB-21	1.10	101.10	2.0047	1165.65	2336.8149

Source: ArcMap 10.8 and MS Excel analysis

SB	48.64×Log of 100+F_f×4919.8 (A)	Log of R_c×1337.77 (B)	Log C_c× 1165.65 (C)	SPR (A-B-C) (D)	Log D (SPR)
SB-1	5017.1711	2678.5134	2335.6439	3.0138	0.4790
SB-2	5017.2566	2678.1302	2335.3385	3.7878	0.5783
SB-3	5017.1814	2677.5953	2336.8381	2.7480	0.439
SB-4	5017.1853	2678.5940	2335.3527	3.2386	0.5103
SB-5	5017.1275	2678.7862	2334.8256	3.5157	0.546
SB-6	5017.1767	2677.6300	2335.8357	3.7110	0.5694
SB-7	5017.1626	2678.4644	2336.1868	2.5113	0.3998
SB-8	5017.1406	2677.5822	2337.3387	2.2197	0.3462
SB-9	5017.1502	2679.0528	2334.6335	3.4639	0.5395
SB-10	5017.1493	2678.2296	2336.3062	2.6136	0.4172
SB-11	5017.1729	2677.8180	2336.2926	3.0622	0.486
SB-12	5017.1470	2677.8655	2336.3084	2.9731	0.4732
SB-13	5017.1517	2678.4375	2335.5913	3.1228	0.4945
SB-14	5017.1443	2677.9180	2336.3184	2.9078	0.4635
SB-15	5017.0977	2678.2064	2335.8669	3.0243	0.4806
SB-16	5017.1656	2677.6304	2336.5878	2.9474	0.4694
SB-17	5017.1559	2678.1996	2336.3372	2.6191	0.4181
SB-18	5017.1747	2678.3940	2335.4342	3.3465	0.5245
SB-19	5017.1560	2678.0012	2336.1868	2.9681	0.4724
SB-20	5017.1982	2678.7273	2335.3363	3.1345	0.4961
SB-21	5017.1320	2677.3084	2336.8149	3.0087	0.4783
Total					10.0813
Average					0.480062

Table 3D Sub-basin Sediment Production Rate (SPR) $\mathrm{Log(SPR)} = 4919.80 + 48.64\log(100 + \mathrm{Ff}) - 1337.77\log(100 + \mathrm{Rc}) - 1165.65\log(100 + \mathrm{Cc})$

Source: ArcMap 10.8 and MS Excel analysis

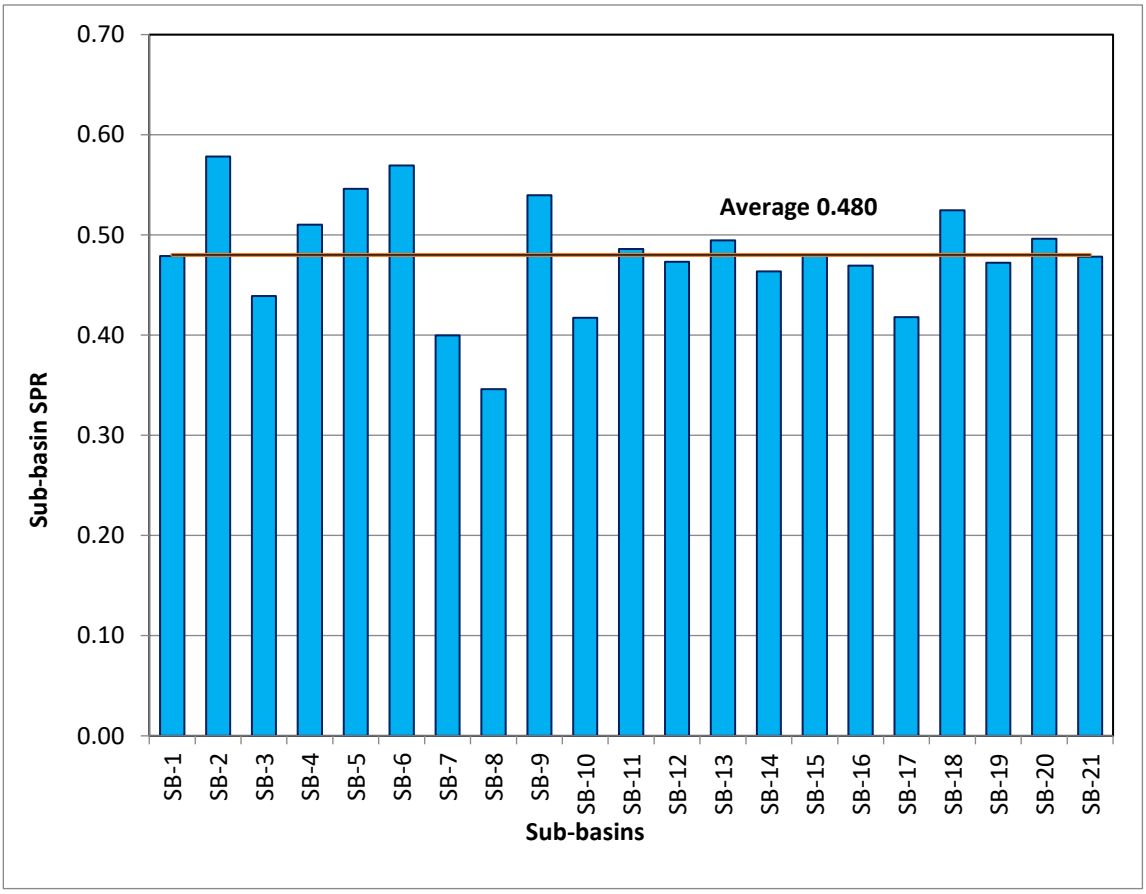

Figure 5 Showing sub-basins Sediment Production Rate (SPR) of Kunhar river basin.

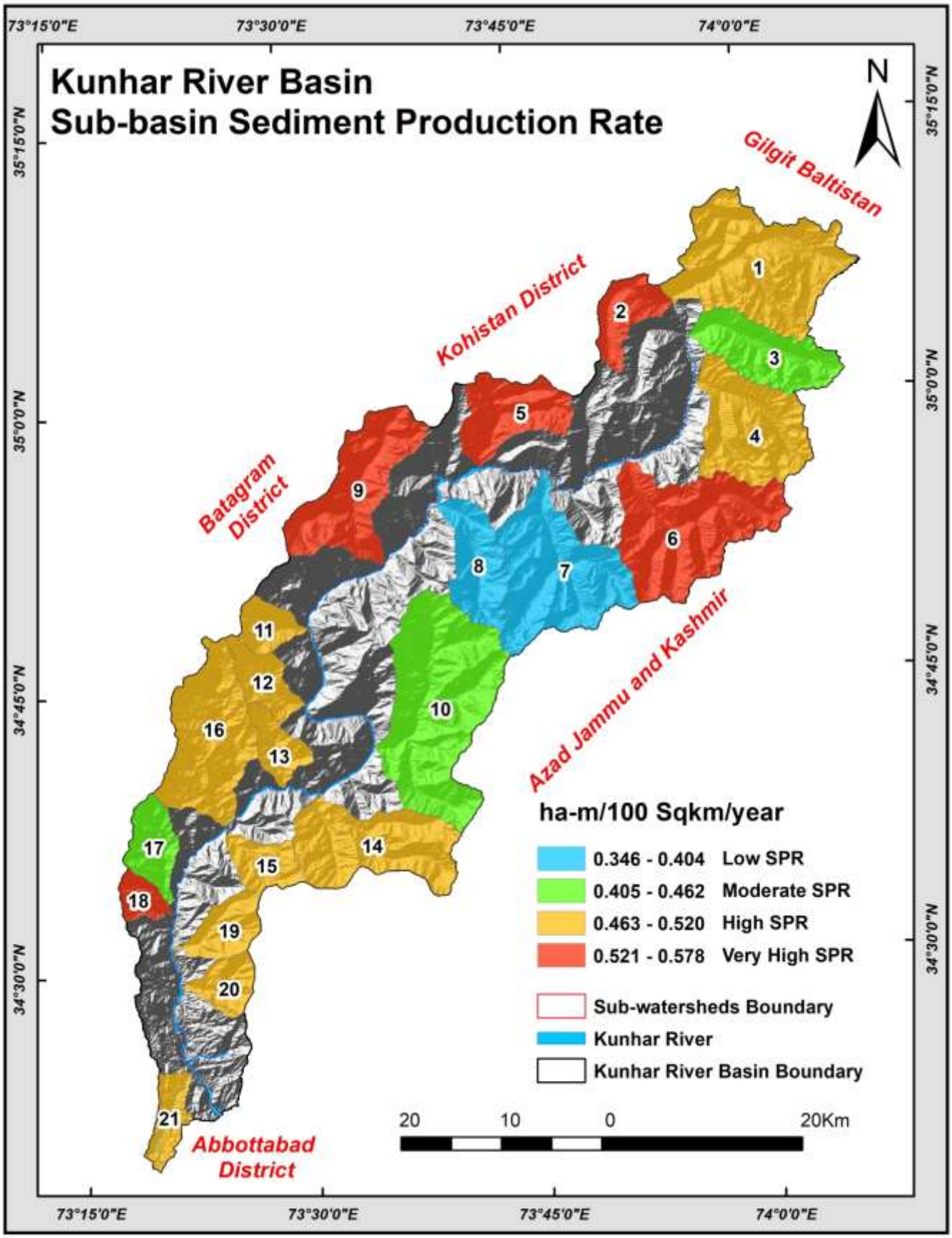

Figure 6 illustrating the sub-basins Sediment Production Rate (SPR) of Kunhar river basin.

5.2 Validation of results

To validate the analysis results of both the sub-basin soil erosion susceptibility by compound factor approach and sediment production rate approach a comparative analysis was made between the sediment production rate approach and rate of soil erosion estimated through the RUSLE model by Hafizullah (2022). Figure 7A illustrates the results of the sediment production rate analysis, while 7B represents the results of the RUSLE model. For the analysis, the RUSLE estimated soil erosion rate was derived at the sub-basin level in ArcMap 10.8. for this purpose the RUSLE-based soil erosion map was overlaid by a sub-basin boundary and through the zonal statistics tool in ArcMap Spatial analyst the zonal statistics as table was computed using input raster or feature zone data as sub-basin layer and input value raster as RUSLE based rate of soil erosion map. Subsequently, the table was created showing the sub-basin-wise rate of soil erosion. Figure 7B is the result of the analysis.

The analysis reveals that sub-basins SB-6 and SB-9 which were classified as very high sediment-producing sub-basins by sediment production rate analysis were also the ones that were identified as high sediment erosion rate sub-basins by the RUSLE model. Similarly, SB-1 classified as a high sediment-producing sub-basin is also the one that has a high rate of soil erosion in the RUSLE model. The comparison between RUSLE and the sediment production rate approach suggests that sub-basins SB-6 and SB-9 have the highest susceptibility to soil erosion and sediment rate production.

However, there are some dissimilarity as well for instance SB-3 and SB-7 identified as sub-basins very highly susceptible to soil erosion were classified as sub-basins with low sediment production rates. Similarly, SB-8, SB-9, and SB-17 identified as highly susceptible to soil erosion by compound factor approach were classified as sub-basins with Low to moderate sediment production rates.

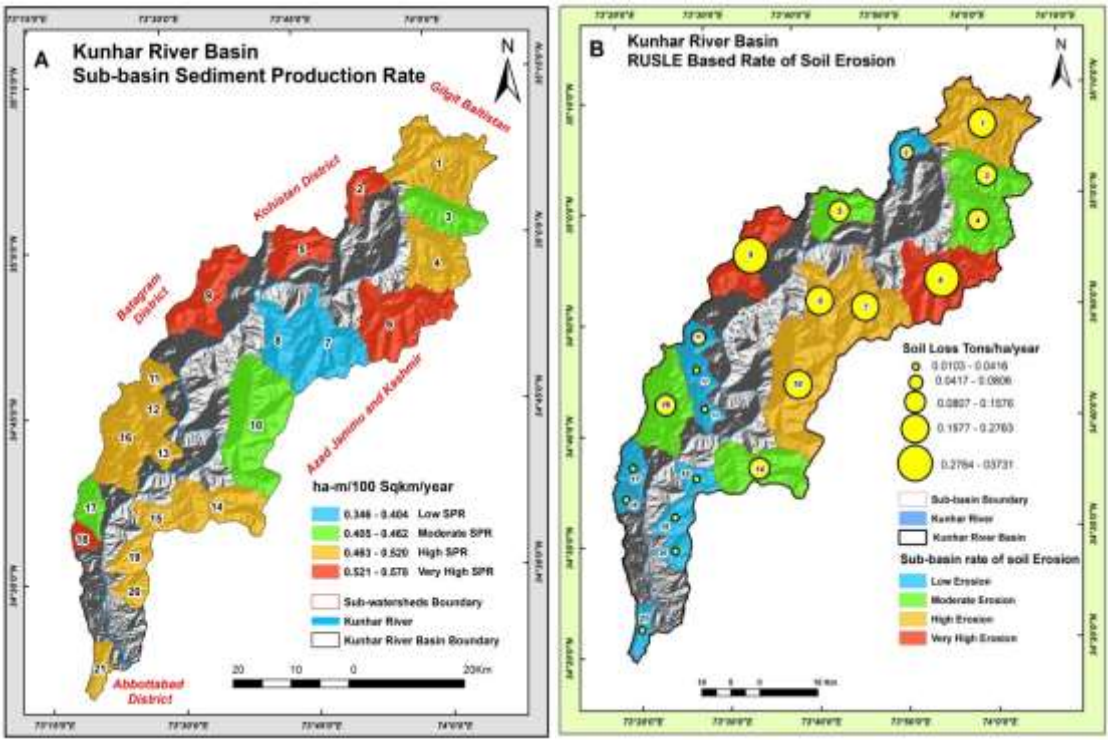

Figure 7 ***(A)*** Illustrating the sub-basin sediment production Rate estimated by current study and ***(B)*** Rate of annual soil loss estimated based on RUSLE Model

Conclusion

Several researches have highlighted the issue of soil erosion in the study region, the Kunhar River basin. However, these investigations relied primarily on the analysis of sedimentation data obtained from Pakistan's Water and Power Development Authority (WAPDA). most of the studies suggest that the KRB has the highest sediment yield in Pakistan. The current study aims to analyze the sediment production rate (SPR) from the KRB in Mansehra district. This study used the SPR approach combined with a geographic information system to evaluate sediment yield in the KRB. The study's findings demonstrate that sediment production occurs in practically every sub-basin of Kunhar River basin. The analysis reveals that the sediment production from KRB is ranging from 0.346 to 0.578 ha-m/100 km^2/year (0.578 meters sediment produced over an area of 10,000 hectares (100 km^2) within a year.).

The analysis suggests that there is a very high sediment production rate in five sub-basins i.e. Sb-2, SB5, SB-6, SB-9, and SB-18; these five sub-basins make up 24 percent of the total Kunhar river sub-basins. Likewise, 11 sub-basins (representing 52% of the Kunhar river sub-basins) namely SB-1, SB-4, SB-11, SB-12, SB-13, SB-14, SB-15, SB-16, SB-19, SB-20, and SB-21 have reported high levels of sediment production. Of the entire Kunhar river sub-basins, two sub-basins SB-7 and SB-8, have a moderate sediment production rate (10% of the sub-basins); the other three, SB-3, SB-10, and SB-17, account for 14% of the sub-basins and have a low sediment production rate.

Pakistan's agricultural sector is strongly reliant on water resources, with surface water accounting for half of total supply. Mangla Dam, located on the Jhelum River, is one of the country's most important water reservoirs. Sedimentation, caused by soil erosion in the dam's catchment area, is an ongoing challenge, gradually decreasing the dam's water-holding capacity. Originally completed in 1967 with a storage capacity of 5.88 million acre-feet (MAF), sedimentation had reduced that capacity to 4.6 MAF by 2004.

The study results are perceived to be helpful for policy makers and other relevant organizations for the effective decision making to combat soil erosion. This study adds to our overall understanding of sediment flows in fluvial systems and their consequences for ecosystem wellness, water quality, and infrastructure management. By quantifying sediment production rates, policymakers and stakeholders can make more informed decisions about land use planning, flood risk mitigation, and sustainable resource management in the Kunhar River basin and similar hydrological systems around the country. In summary, the Kunhar River basin sediment production rate analysis is a first step toward comprehensive watershed management methods aimed at protecting the ecological integrity and socioeconomic resilience of this critical riverine ecosystem.

References

Abboud, I. A., & Nofal, R. A. (2017). Morphometric analysis of wadi Khumal basin, western coast of Saudi Arabia, using remote sensing and GIS techniques. Journal of African Earth Sciences, 126, 58-74.

Achu, A. L., & Thomas, J. (2023). Soil erosion and sediment yield modeling in a tropical mountain watershed of the southern Western Ghats, India using RUSLE and Geospatial tools. Total Environment Research Themes, 8, 100072.

Akbar, H., & Gheewala, S. H. (2020).Changes in hydroclimatic trends in the Kunhar River Watershed. Journal of Sustainable Energy & Environment, 11, 31-41.

Arabameri, A., Pradhan, B., Rezaei, K., Yamani, M., Pourghasemi, H. R., & Lombardo, L. (2018).Spatial modelling of gully erosion using evidential belief function, logistic regression, and a new ensemble of evidential belief function–logistic regression algorithm. Land Degradation & Development, 29(11), 4035-4049.

Batool, S., Shirazi, S. A., & Mahmood, S. A. (2021). Appraisal of soil erosion through RUSLE model and hypsometry in Chakwal Watershed (Potwar-Pakistan). Sarhad Journal of Agriculture, 37(2), 594-606.

Benzougagh, B., Meshram, S. G., Dridri, A., Boudad, L., Baamar, B., Sadkaoui, D., &Khedher, K. M. (2022).Identification of critical watershed at risk of soil erosion using morphometric and geographic information system analysis. Applied Water Science, 12, 1-20.

Bharath, A., Kumar, K. K., Maddamsetty, R., Manjunatha, M., Tangadagi, R. B., & Preethi, S. (2021). Drainage morphometry based sub-watershed prioritization of Kalinadi basin using geospatial technology. Environmental Challenges, 5, 100277.

Buccolini, M., Coco, L., Cappadonia, C., & Rotigliano, E. (2012). Relationships between a new slope morphometric index and calanchi erosion in northern Sicily, Italy. Geomorphology, 149, 41-48.

Das, B., Bordoloi, R., Thungon, L. T., Paul, A., Pandey, P. K., Mishra, M., & Tripathi, O. P. (2020). An integrated approach of GIS, RUSLE and AHP to model soil erosion in West Kameng watershed, Arunachal Pradesh. Journal of Earth System Science, 129, 1-18.

Fenta, A. A., Yasuda, H., Haregeweyn, N., Belay, A. S., Hadush, Z., Gebremedhin, M. A., & Mekonnen, G. (2017). The dynamics of urban expansion and land use/land cover changes using remote sensing and spatial metrics: the case of Mekelle City of northern Ethiopia. International journal of remote sensing, 38(14), 4107-4129.

Flanagan, D. C., & Nearing, M. A. (1995). USDA-Water Erosion Prediction Project: Hillslope profile and watershed model documentation. USDA-ARS National Soil Erosion Research Laboratory West Lafayette, Indiana, 10, 1-123.

Foster, G. R., & Wischmeier, W. (1974). Evaluating irregular slopes for soil loss prediction. Transactions of the ASAE, 17(2), 305-0309. Geomorphology, 398, 108064.

Ganie, P. A., Posti, R., Kunal, K., Kunal, G., Bharti, V. S., Sehgal, V. K., ... & Pandey, P. K. (2023). Modelling of the Himalayan Mountain river basin through hydro-morphological and compound factor-based approaches using geoinformatics tools. Modeling Earth Systems and Environment, 9,3053–3084.

Ghabbour, E. A., Davies, G., Misiewicz, T., Alami, R. A., Askounis, E. M., Cuozzo, N. P., ...& Shade, J. (2017). National comparison of the total and sequestered organic matter contents of conventional and organic farm soils. Advances in Agronomy, 146, 1-35.

Khan, H. (2021). Soil Erosion Susceptibility and Soil Loss Estimation Kunhar River Watershed, District Mansehra, Pakistan. MPhil Thesis submitted to Department of Geography and Geomatics, University of Peshawar.

Haokip, P., Khan, M. A., Choudhari, P., Kulimushi, L. C., &Qaraev, I. (2022). Identification of erosion-prone areas using morphometric parameters, land use land cover and multi-criteria decision-making method: geo-informatics approach. Environment, Development and Sustainability, 24(1), 527-557.

Haregeweyn, N., Poesen, J., Nyssen, J., De Wit, J., Haile, M., Govers, G., &Deckers, S. (2006). Reservoirs in Tigray (Northern Ethiopia): characteristics and sediment deposition problems. Land degradation & development, 17(2), 211-230.

Hembram, T. K., & Saha, S. (2020). Prioritization of sub-watersheds for soil erosion based on morphometric attributes using fuzzy AHP and compound factor in Jainti River basin, Jharkhand, Eastern India. Environment, Development and Sustainability, 22(2), 1241-1268.

Horton, R. E. (1945). Erosional development of streams and their drainage basins; hydrophysical approach to quantitative morphology. Geological society of America bulletin, 56(3), 275-370.

Jahun, B. G., Ibrahim, R., Dlamini, N. S., & Musa, S. M. (2015). Review of soil erosion assessment using RUSLE model and GIS. Journal of Biology, Agriculture and Healthcare, 5(9), 36-47.

Kacem, L., Igmoullan, B., Mokhtari, S., Amar, H., & Agoussine, M. B. (2014). Morphometric characterization of upstream mountainous watershed using geographic information system GIS: high valley of Tifnoute High Moroccan Atlas. Journal of Biodiversity and Environmental Sciences, 5(6), 62-66.

Kulimushi, L. C., Choudhari, P., Maniragaba, A., Elbeltagi, A., Mugabowindekwe, M., Rwanyiziri, G., ...& Singh, S. K. (2021). Erosion risk assessment through prioritization of sub-watersheds in Nyabarongo River catchment, Rwanda. Environmental Challenges, 5, 100260.

Li, Z., & Fang, H. (2016). Impacts of climate change on water erosion: A review. Earth-Science Reviews, 163, 94-117.

Li, Z., Wang, S., Song, S., Wang, Y., &Musakwa, W. (2021).Detecting land degradation in Southern Africa using time series segment and residual trend (TSS-RESTREND). Journal of Arid Environments, 184, 104314.

Mahmood, R., Jia, S., & Babel, M. S. (2016). Potential impacts of climate change on water resources in the Kunhar River Basin, Pakistan. Water, 8(1), 23.

Mahmood, R., Babel, M. S., & Shaofeng, J. I. A. (2015). Assessment of temporal and spatial changes of future climate in the Jhelum river basin, Pakistan and India. Weather and Climate Extremes, 10, 40-55.

Maqsoom, A., Aslam, B., Hassan, U., Kazmi, Z. A., Sodangi, M., Tufail, R. F., & Farooq, D. (2020). Geospatial assessment of soil erosion intensity and sediment yield using the revised universal soil loss equation (RUSLE) model. ISPRS International Journal of Geo-Information, 9(6), 356.

Merritt, W. S., Letcher, R. A., & Jakeman, A. J. (2003). A review of erosion and sediment transport models. Environmental modelling & software, 18(8-9), 761-799.

Meshram, S. G., Singh, V. P., Kahya, E., Alvandi, E., Meshram, C., & Sharma, S. K. (2020). The feasibility of multi-criteria decision making approach for prioritization of sensitive area at risk of water erosion. Water Resources Management, 34, 4665-4685.

Miller, V. C. (1953). Quantitative geomorphic study of drainage basin characteristics in the Clinch Mountain area, Virginia and Tennessee. Technical report (Columbia University. Department of Geology); no. 3.

Mishra, A. K., Upadhyay, A., Mishra, P. K., Srivastava, A., & Rai, S. C. (2023). Evaluating geo-hydrological environs through morphometric aspects using geospatial techniques: A case study of Kashang Khad watershed in the Middle Himalayas, India. Quaternary Science Advances, 11, 1-10.

Misra, N., Satyanarayana, T., & Mukherjee, R. K. (1984). Effect of top elements on the sediment production rate from Sub-watershed in Upper Damodar Valley. J Agric Eng, 21(3), 65-70.

Mitasova, H., & Iverson, L. (1992). Erosion and sedimentation potential analysis for Hunter lake. An environmental assessment of the Hunter Lake project area, edited by WU Brigham, and AR Brigham (Illinois Natural History Survey Champaign, Illinois).

Moore, I. D., & Burch, G. J. (1986). Modelling erosion and deposition: topographic effects. Transactions of the ASAE, 29(6), 1624-1630.

Moore, I. D., & Wilson, J. P. (1992). Length-slope factors for the Revised Universal Soil Loss Equation: Simplified method of estimation. Journal of soil and water conservation, 47(5), 423-428.

Morgan, R. P. C., Quinton, J. N., Smith, R. E., Govers, G., Poesen, J. W. A., Auerswald, K., ... & Styczen, M. E. (1998). The European Soil Erosion Model (EUROSEM): a dynamic approach for predicting sediment transport from fields and small catchments. Earth Surface Processes and Landforms: The Journal of the British Geomorphological Group, 23(6), 527-544.

Nasir, M. J., Ahmad, W., Jun, C., Iqbal, J., & Bateni, S. M. (2023). Soil erosion susceptibility assessment of Swat River sub-watersheds using the morphometry-based compound factor approach and GIS. Environmental Earth Sciences, 82(12), 315.

Panagos, P., Standardi, G., Borrelli, P., Lugato, E., Montanarella, L., &Bosello, F. (2018). Cost of agricultural productivity loss due to soil erosion in the European Union: From direct cost evaluation approaches to the use of macroeconomic models. Land Degradation & Development, 29(3), 471-484.

Pande, C., Moharir, K., & Pande, R. (2021). Assessment of morphometric and hypsometric study for watershed development using spatial technology–a case study of Wardha river basin in Maharashtra, India. International Journal of River Basin Management, 19(1), 43-53.

Prakash, K., Rawat, D., Singh, S., Chaubey, K., Kanhaiya, S., & Mohanty, T. (2019). Morphometric analysis using SRTM and GIS in synergy with depiction: a case study of the Karmanasa River basin, North central India. Applied Water Science, 9(1), 13-23.

Pham, T. G., Degener, J., &Kappas, M. (2018). Integrated universal soil loss equation (USLE)and Geographical Information System (GIS) for soil erosion estimation in A Sap basin: Central Vietnam. International Soil and Water Conservation Research, 6(2), 99-110.

Rai, P. K., Mishra, V. N., & Mohan, K. (2017). A study of morphometric evaluation of the Son basin, India using geospatial approach. Remote Sensing Applications: Society and Environment, 7, 9-20.

Rumpel, C. (2022). Interactions between soils and climate change,Reference Module in Earth Systems and Environmental Sciences. Elsevier. https://doi.org/10.1016/B978-0-12-822974-3.00035-5.

Sabir, M. A., Shafiq-Ur-Rehman, S., Umar, M., Waseem, A., Farooq, M., & Khan, A. R. (2013). The Impact of Suspended Sediment Load on Reservoir Siltation and Energy Production: a Case Study of the Indus River and Its Tributaries. Polish Journal of Environmental Studies, 22(1).

Saha, A., Ghosh, P., &Mitra, B. (2018). GIS based soil erosion estimation using RUSLE model: a case study of upper Kangsabati watershed, West Bengal, India. International Journal of Environmental Sciences & Natural Resources, 13(5), 119-126.

Singh, O., & Singh, J. (2018). Soil erosion susceptibility assessment of the lower Himachal Himalayan Watershed. Journal of the Geological Society of India, 92, 157-165.

Smith, D. D., & Wischmeier, W. H. (1957). Factors affecting sheet and rill erosion. Eos, Transactions American Geophysical Union, 38(6), 889-896.

Strahler, A. N. (1964). Quantitative geomorphology of drainage basin and channel networks. Handbook of applied hydrology.

Sukristiyanti, S., Maria, R., & Lestiana, H. (2018, February). Watershed-based morphometric analysis: a review. In IOP conference series: earth and environmental science (Vol. 118, No. 1, p. 012028). IOP Publishing.

Todorovski, L., & Džeroski, S. (2006). Integrating knowledge-driven and data-driven approaches to modeling. ecological modelling, 194(1-3), 3-13.

Tsegaye, B. (2019). Effect of land use and land cover changes on soil erosion in Ethiopia. International Journal of Agricultural Science and Food Technology, 5(1), 026-034.

Ullah, S., Ali, A., Iqbal, M., Javid, M., & Imran, M. (2018). Geospatial assessment of soil erosion intensity and sediment yield: a case study of Potohar Region, Pakistan. Environmental Earth Sciences, 77(19), 1-13.

Vinutha, D. N., & Janardhana, M. R. (2014). Morphometry of The payaswini watershed, coorg district, karnataka, India, using remote sensing and GIS techniques. International Journal of Innovative Research in Science, Engineering and Technology, 3(5), 516-524.

Wang, J., Wei, H., Cheng, K., Ochir, A., Davaasuren, D., Li, P &Nasanbat, E. (2020).Spatio-temporal pattern of land degradation from 1990 to 2015 in Mongolia. Environmental Development, 34, 100497.

Williams, J. R. (1985). Physical components of the EPIC model. Soil Erosion and Conservation. Soil Conservation Society of America, Ankeny, Iowa. 1985. p 272-284,

Wilson, J. J., Chandrasekar, N., & Magesh, N. S. (2012). Morphometric analysis of major sub-watersheds in Aiyar & Karai Pottanar Basin, Central Tamil Nadu, India using remote sensing & GIS techniques. Bonfring International Journal of Industrial Engineering and Management Science, 2(1), 8-15.

Wischmeier, W. H., & Smith, D. D. (1978). Predicting rainfall erosion losses: a guide to conservation planning (No. 537).Department of Agriculture, Science and Education Administration.